Information Processing and Management 59 (2022) 102741

Contents lists available at ScienceDirect

Information Processing and Management

journal homepage: www.elsevier.com/locate/infoproman

A new data mining method for time series in visual analysis of regional economy

Yang Bai [a], Min Zhao [a], Rong Li [b], Peizhu Xin [a,*]

[a] Business School, Hohai University, Nanjing 211100, China
[b] Foreign Language School, Hohai University, Nanjing 211100, China

ARTICLE INFO

Keywords:
Time series
Regional economy
Visualization

ABSTRACT

In order to improve the effect of visual analysis of regional economy, this paper uses machine learning algorithms to analyze time series data, uses various models and methods of intelligent data analysis to mine data laws from huge data, statistical data reports, and find problems in economic development. Moreover, this paper combines the time series algorithm to design and plan the functional structure of the system, and design a separate module structure from the actual situation of regional economic analysis, and build a model system from the overall structure. After constructing the system, this paper tests the system. From the results of the experimental research, we can see that the regional economic visualization system based on time series constructed in this paper has perfect system functions and can meet the needs of regional economic analysis.

1. Introduction

The safe layout of economic analysis work is related to the basis of the overall situation, and the analysis and processing of analysis data is the direct purpose of the analysis work. At this stage, there is a big gap between the analysis of economic data in our country's statistical institutions and that of foreign countries. The research on economic data analysis in most developed countries such as Europe and the United States has entered the stage of web applications, data warehouse applications, and intelligent data analysis technology applications. However, China's statistical agencies have not applied intelligent data analysis technology to economic data analysis, but simply use network technology and database technology to obtain some results. The reason is that, on the one hand, China's scientific analysis and application of relevant data results are only in the research stage. On the other hand, intelligent data analysis methods are new technologies for processing massive data that have only been developed in recent years.

The results of economic data analysis not only help the country and governments at all levels understand the basic national conditions and strength of our country, but also provide an important basis for the country and governments at all levels to formulate national economic development plans and guide the formulation of macroeconomic decisions. At the same time, it can provide detailed data support for further adjustment and optimization of the economic structure and implementation of the transformation of macroeconomic policies. Therefore, how to scientifically carry out analysis work and how to analyze the results of statistical analysis will be of great significance. The traditional analysis workflow is: preliminary preparation for economic analysis, analysis and publicity, analyst training, analyst publication and receipt, manual review and entry, program review, return of errors, re-modification of the

* Corresponding author.
E-mail address: xinpeizhu@hhu.edu.cn (P. Xin).

https://doi.org/10.1016/j.ipm.2021.102741
Received 28 June 2021; Received in revised form 28 August 2021; Accepted 29 August 2021
Available online 24 September 2021
0306-4573/© 2021 Elsevier Ltd. All rights reserved.

investigation unit, re-review of the program, and summary reporting. Traditional working methods have become overwhelmed in the context of the continuous economic development and the increasing number of adjustments in the analysis process, and too many manual operations have more chances of error, and will cause work lag. Therefore, analysis work needs to rely on Internet technology to carry out network data transmission, and use intelligent data analysis methods or data mining methods to analyze data results.

With the rapid and multi-directional economic growth, China has achieved world-renowned achievements in economic, political, and cultural aspects. However, this kind of rapid growth is based on huge energy consumption and resource occupation, which is detrimental to the maintenance and sustainability of resources and the maintenance and optimization of environmental carrying capacity. This development model is not in line with the concept of sustainable development and cannot be maintained for a long time. In order to solve the above problems, the concept of low-carbon economy came into being. Low-carbon economy is a sustainable, environmentally friendly, and green economic model, and it is the inevitable trend and ultimate destination of economic development. However, the relevant research on low-carbon economy is not comprehensive, its understanding is not perfect, its development model, evaluation reference, development method and trend are not perfect, and scientific and systematic assessment is still very difficult (Montford & Goldsmith, 2016).

In recent years, the development of computer technology has allowed us to use more intuitive visualization techniques to demonstrate China's multi-dimensional evaluation system for the low-carbon economy. The development of computer graphics and the advancement of visualization technology have made information visualization more and more common. Through visualization, various non-image information can be graphed, the ability to understand and analyze information can be improved, and data storage space can be reduced. At the same time, data and information can be interactively processed to strengthen in-depth information mining. In addition, the visualization of the data calculation process and the visualization of temporal data can enhance people's ability to monitor real-time information, increase the probability of risks and unnecessary hazards, and reduce the loss caused by unfavorable dynamic changes (Wanjohi et al., 2017).

After constructing the framework of China's low-carbon economic evaluation visualization platform, through computer and visualization technology, the visualization of low-carbon economic evaluation can be realized, and the scientific, systematic and diversified evaluation of the low-carbon economic development level can be promoted. Generally, the visualization platform of the evaluation system has generality and versatility. The framework of the low-carbon economic evaluation visualization platform can be used directly or through appropriate improvements to realize the visualization platform of other related evaluation systems, which provides a certain model reference for its structure and function realization (Magendans et al., 2017).

Based on machine learning and time series algorithms, this paper studies the visual analysis of regional economy, constructs a corresponding system, and validates the system algorithm with experimental analysis.

2. Related work

Visual simulation technology refers to a more intuitive simulation realization method that transforms digital (data) information into a variety of images that can change with time and space. Its key technical means are: visualization algorithm, image generation, human-computer interaction, rendering, virtual reality, effect evaluation and modeling technology (Cole et al., 2014). For the visual simulation of some non-visual physical quantities, the core technology is to visually display the three-dimensional physical field through the three-dimensional data field obtained by calculation. There are two main methods. One is to draw isosurfaces generated by 3D data to represent 3D physical fields, such as slicing technology, meshing, and ensemble deformation surface method. The second is a visualization method based on projection to project three-dimensional data onto the screen, and its representative technologies include direct projection and ray tracing. The literature (Zalik, 2015) developed a comprehensive underwater acoustic simulation system to model and simulate underwater acoustic signals, and the literature (Lucarelli et al., 2015) developed a virtual system used to simulate the driving environment of an underwater vehicle. At present, the development of visual simulation is broader, and its development trend is that the modeling methods are becoming more and more diversified, and the performance components are becoming more and more combined, virtualized and repetitive. Therefore, a model assembly technology based on component library is proposed. It uses a structured idea to first establish a database of components, and then select, combine, and components in the component library according to the model to be built to achieve rapid modeling (Chan, 2015). However, there are still some shortcomings in this method that need to be improved, such as the standardization and consistency of components, and the fineness of models. With the increasing complexity and functionality of visual simulation systems, traditional development methods are becoming more and more difficult to adapt. Therefore, a new research direction at present is to design a visualization platform system with good scalability, relatively high function integration, and high reusability. The literature (West & Worthington, 2014) proposed a general visual simulation system development technology, which first abstracts the scene, extracts meta-models, and then establishes a simulation system through these meta-models. The literature (Tanimura et al., 2014) put forward five visual evaluation indicators such as detail description and picture elements, and evaluated the simulation system based on the fuzzy evaluation method. The literature (Scharding, 2015) used nine visual evaluation indicators such as brightness, contrast, and resolution to evaluate the simulation system. The literature (Su & Furman, 2017) proposed to use the fuzzy analytic hierarchy process to evaluate the simulation system, and choose the visual evaluation index from the aspects of three-dimensional model development, virtual environment construction, and screen display. However, the evaluation of the simulation visualization system needs further research.

Visualization is developed with the development of computer intelligence technology and the emergence of intelligent terminals. At first, the visualization technology in scientific computing was regarded as the visualization technology. The visualization technology in scientific computing refers to the product of the combined effect of graphics and computer image processing. It displays the calculation data in scientific research, the data obtained by measurement and the calculation data related to engineering on the

computer monitor in the form of images and graphics, and combines the functions of human-computer interaction (Guo et al., 2021). The literature (Karanikić et al., 2019) recommended scientific visualization as a task for future research. Since then, scientific visualization has gradually replaced the term visualization in scientific computing. In recent years, foreign research on visualization has mainly focused on the research of visualization systems, the formulation and standardization of visualization evaluation indicators, the optimization of visualization algorithms, breakthroughs in visualization technology, and visualization methods and methods (Ataka, 2014).

Research results are mainly concentrated in the fields of computer software and computer applications, physical geography and surveying and mapping, automation technology and power industry, and the research level is concentrated in the field of engineering technology and basic and applied basic research (Ataka, 2014). With the advent of the big data era, the amount of geospatial data has grown rapidly. Moreover, data types and data sources are becoming more and more diverse, such as text data, spatiotemporal data, structured data, unstructured data, metaphor data in the network, social network data, trajectory data, recorded data, video and audio data, life services data etc. How to quickly sort out the internal and temporal relationships between various data in a short period of time, and to query, search for the data we need, and share data with others has become a problem faced by researchers (Barde, 2015). Visualization will perfectly solve this problem, and improve the efficiency of obtaining information in a way that conforms to the cognitive form and personal cognitive habits. Visualization is to process and convert data such as text, network, video and audio into visualized structured data, and display the visualized structured data on its display screen through computer display technology. After that, the researcher can consult, browse and manipulate the view results of the view interface through the display screen (Ferramosca et al., 2014).

3. Time series function based on machine learning

In theory, any finite function that satisfies the following two formulas can be used as a mother wavelet, but in fact, the choice of mother wavelet is principled. First, the mother wavelet must have compact support, and it is also a regular real or complex function. In this way, the wavelet mother function can be localized in the time and frequency domains, which can meet the requirements of time-frequency analysis .The wavelet function $\varphi(x)$ satisfies the following two basic conditions (Zhou et al., 2014).:

1) The integral of $\varphi(x)$ is zero.

$$\int_R \varphi(x) d(x) = 0 \tag{1}$$

2) The square integral of $\varphi(x)$ is 1.

$$\int_R \varphi^2(x) d(x) = 1 \tag{2}$$

By scaling and panning the mother wavelet $\varphi(x)$, many copies of the same shape but different widths and positions can be obtained. For example, it can be expanded and panned according to the following formula (Bhattacharya et al., 2019):

$$\varphi_{a,b}(x) = |a|^{-1/2} \varphi((x-b)/a) \tag{3}$$

$\varphi_{a,b}(x)$is called the wavelet basis function. Among them, a is the scale function or expansion parameter, and b is the displacement parameter. By changing a, the scale and range of the function can be changed, and by changing the value of b, it is equivalent to changing the time window displacement and instant window center of the function, which affects the analysis result of the function around point b, as shown in the following figure (Li et al., 2021).

It can be seen from the figure that not only the wavelet has energy localization characteristics in the time domain and frequency domain, but also the wavelet function after scaling and translation also has the energy localization characteristics in the time domain and frequency domain.In addition, it can be roughly seen from the figure how the expansion and displacement parameters affect the shape of the wavelet basis function. Therefore, it can be seen that the scaling parameter controls the scaling of the function. When the expansion parameter a increases, the wavelet function is stretched and the waveform becomes wider, that is, the time window of the function becomes wider. If the expansion parameter a decreases, the wavelet function is compressed, and the waveform in the figure becomes narrower, that is, the time window of the function becomes narrower. The movement of the displacement parameter b is the center position of the time window as a function of influence (Vu et al., 2019).

According to the method of measuring the position and scale of the window, the waveform reference of the time window and frequency window of the wavelet base is defined as follows:

1) Time window center: In fact, the time window center is the first moment of the calculated signal in the time domain:

$$t_0 = \frac{\int_{-\infty}^{\infty} t\left|\varphi_{a,b}(t)\right|^2 dt}{\| \varphi_{a,b}(t) \|^2} = \frac{\int_{-\infty}^{\infty} t\left|\varphi_{a,b}(t)\right|^2 dt}{\int_{-\infty}^{\infty} \left|\varphi_{a,b}(t)\right|^2 dt} \tag{4}$$

2) Time window width: the time domain standard deviation of the calculation signal:

$$\sigma_1 = \frac{\left[\int_{-\infty}^{\infty} (t-t_0)^2 \left|\varphi_{a,b}(t)\right|^2 dt\right]^{1/2}}{\| \varphi_{a,b}(t) \|} \tag{5}$$

3) The center of the frequency window: the first moment of the calculation signal in the frequency domain:

$$\omega_0 = \frac{\int_{-\infty}^{\infty} \omega \left|\varphi_{a,b}(\omega)\right|^2 d\omega}{2\pi \| \varphi_{a,b}(\omega) \|^2} \tag{6}$$

4) Frequency window width: the frequency domain standard deviation of the calculation signal:

$$\sigma_\omega = \frac{\left[\frac{1}{2\pi}\int_{-\infty}^{\infty} (\omega-\omega_0)^2 \left|\varphi_{a,b}(t)\right|^2 d\omega\right]}{\| \varphi_{a,b}(\omega) \|} \tag{7}$$

We set the mother wavelet as $\varphi(x)$ and its Fourier transform as $\varphi(\omega)$. According to the above formula, we deduced that the waveform parameters corresponding to the mother wavelet $\varphi(x)$ are $t_0^{'}, \sigma_t^{'}, \omega_0^{'}, \sigma_\omega^{'}$ respectively, and the waveform parameters corresponding to the wavelet basis function $\varphi_{a,b}(t)$ after expansion and contraction are $t_0, \sigma_t, \omega_0, \sigma_\omega$ respectively. From this, the following conclusions can be drawn (Teljeur et al., 2014).

1) The nature of energy conservation can ensure that the energy of the wavelet base at different positions is equal, and the wavelet transform result will not introduce additional noise energy.

$$E = \| \varphi_{a,b}(t) \|^2 = \| \varphi(t) \|^2 \tag{8}$$

$$\| \varphi_{a,b}(\omega) \|^2 = \| \varphi(\omega) \|^2 \tag{9}$$

2) The center position of the window is affected by the moderate factor and the displacement factor at the same time.

$$t_0 = at^{/prime} + \tau \tag{10}$$

$$\omega_0 = \frac{\omega_0{}^{/prime}}{a} \tag{11}$$

3) The width of the window, that is, the standard deviation is only affected by the expansion and contraction parameters, and the effect is opposite.

$$\sigma_t = a\sigma_t{}^{/prime} \tag{12}$$

$$\sigma_\omega = \frac{\sigma_\omega{}^{/prime}}{a} \tag{13}$$

4) The area remains the same: the time-frequency window stretches and moves on the time-frequency plane, but the total area remains the same.

$$S_w = \sigma_\omega \sigma_t = \sigma_\omega{}^{/prime} \sigma_t{}^{/prime} \tag{14}$$

It can be seen that the waveform parameters of the wavelet basis function will change with the change of scale and displacement. Next, the influence of the expansion and displacement parameters on the time-frequency window will be analyzed in detail (Kleven & Schultz, 2014).

1) Time-frequency window position

It can be seen that when a increases, the center position of the frequency window becomes smaller, the center position of the time window becomes larger, and the time-frequency window moves toward the low frequency, which is mainly used for low frequency analysis. However, when a decreases, the center position of the frequency window becomes larger, the center position of the time window becomes larger, and the time-frequency window moves toward high frequencies, which is mainly used for high-frequency

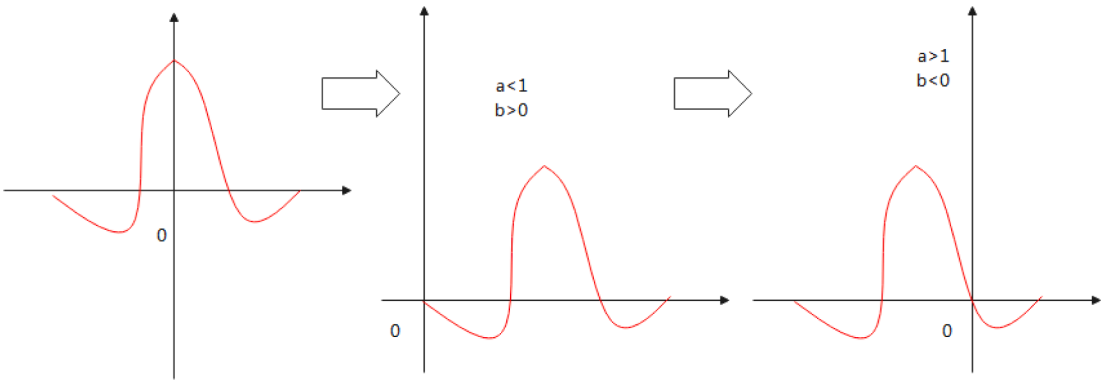

Fig. 1. Wavelet diagram when a and b are changed.

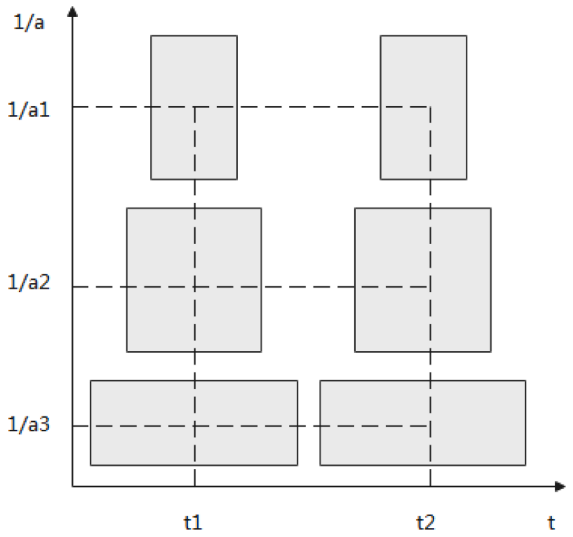

Fig. 2. Wavelet adaptive time-frequency window.

analysis.

2) Time-frequency window size

It can be seen that when a increases, the accuracy of time domain analysis decreases, and the width of the time window becomes larger, the width of the frequency window becomes smaller, the accuracy of frequency domain analysis increases and the frequency band becomes narrower. Moreover, the frequency components falling into the frequency window are reduced, and the information extracted by the wavelet transform $WT_f(a,\tau)$ is narrowband information. However, when a decreases, the accuracy of time-domain analysis increases, and the width of the time window becomes smaller, the width of the frequency window becomes larger, and the accuracy of frequency-domain analysis decreases and the frequency band becomes wider. Moreover, the frequency components that fall into the frequency window increase, and the information extracted by the wavelet transform $WT_f(a,\tau)$ is broadband information (Hoffmann, 2014).

The width of the frequency window and the width of the window change in the opposite direction. The compression of the frequency window will inevitably lead to the stretching of the window, and the stretching of the frequency window will cause the window to compress.Moreover, when the frequency window is stretched and widened, the center of the frequency window also becomes larger. The time window structure of this unique wavelet transform is very in line with the needs of practical applications. When the low-frequency signal lasts for a long time, it is hoped that the time window is as wide as possible and the frequency domain is more detailed. However, when analyzing high-frequency signals, it is always desirable to narrow the time-frequency window, while the frequency domain can appropriately reduce the accuracy. This is what we usually call the adaptive time-frequency window of the wavelet basis function.Figure 1Figure 2 demonstrate the adaptive scaling effect of the wavelet time-frequency window.

In a sense, the expansion function a directly corresponds to the analysis frequency or the center of the frequency window and the analysis accuracy, that is, the width of the frequency window. Therefore, although there is no frequency domain factor w in $WT_f(a,\tau)$, it is essentially a type of time-frequency analysis (Carvalho & Di Guilmi, 2020).

3) Displacement factor

It can be seen that the displacement factor b affects only the position of the time window center. From the perspective of time domain, we know that the displacement will not affect the waveform size. Moreover, from the perspective of the frequency domain, the translation of the function in the time domain will only introduce additional phase in the frequency domain, and will not affect the amplitude-frequency characteristics, and thus will not affect the size and center of the frequency window.

4) Time-frequency window area

When a mother wavelet $\varphi(x)$ is selected, the scale parameter a will affect the time window width σ_t and the frequency window width σ_ω, but the window area $S_w = \sigma_\omega \sigma_t$does not change with the change of a, and the window area always remains a constant. This can also verify that compression and stretching in the time domain will lead to stretching and compression in the frequency domain.

5) Constant quality factor

The wavelet mother function $\varphi(x)$ is a typical band-pass filter, and multiple wavelet basis functions obtained by changing the scale parameter a to translate and stretch can form a variety of band-pass filter groups. Although the position and size of the frequency window of these band-pass filters are variable, the quality factor is indeed constant. In communication digital signal processing, the ratio $Q = \sigma / \omega$ between the bandwidth of the filter and the center frequency is defined as the quality factor. We can know that the quality factor Q_a when the expansion parameter is a is identical to the quality factor Q_a of the mother wavelet. In the expression of the quality factor Q_a of these filters, since there is no influence of the scale factor, this characteristic of constant quality has very good practical value in practical applications.

In theory, as long as it can meet the specific requirements of practical applications, the scale parameter a and the displacement parameter b can be discretely processed in any way. Among them, a more typical and generally accepted discrete method is as follows:

1) The scale parameter a is discretized according to the power series, namely

$$a = a_0^j \tag{15}$$

2) Under the same scale, the displacement factor b is uniformly discretized, namely

$$b = k a_0^j b_0 \tag{16}$$

Among them, j and k are integers, and a_0 is a constant greater than 1. b_0 is a constant greater than 0, and the selection of a and b is related to the specific form of wavelet $\varphi(x)$.

Then the discrete wavelet function is expressed as (Gantino, 2015):

$$\begin{aligned} \varphi_{j,k}(x) &= \left|a_0^j\right|^{-1/2} \varphi\left(\left(t - n b_0 a_0^j\right) / a_0^j\right) \\ &= \left|a_0^j\right|^{-1/2} \varphi\left(a_0^{-j} x - k b_0\right) \end{aligned} \tag{17}$$

The corresponding discrete wavelet transform is expressed as:

$$Wf(j,k) = \left\langle f, \varphi_{j,k} \right\rangle = \int_R f(x) \varphi^*_{j,k}(x) dx \tag{18}$$

When the discretized wavelet transform coefficient $\{Wf(j,k)\}_{j \in R, k \in R}$ is compared with the continuous wavelet transform coefficient $\{Wf(a,b)\}_{a \in R, b \in R}$, it can be seen that the former is a two-dimensional discrete sequence of integers j and k, while the latter is a two-dimensional continuous variable of real numbers a and b.

It should be noted that the discrete scheme is not only the above-mentioned discrete scheme. a and b can be discretized as required according to actual applications.

We set $D = S_2^{d_0} f[n] (n \in Z)$ as the N-point discrete sampling sequence of the original signal f, and $W_2^{d_j} f[n] (n \in Z)$ as the wavelet transform value of D on each scale 2^j, which is called the wavelet coefficient. It refers to the high-pass component of the signal at different scales after wavelet decomposition.

Definition: If the following conditions are met:

$$\left|W_2^{d_j} f[n_i]\right| \geq \left|W_2^{d_j} f[n_i - 1]\right| \tag{19}$$

$$\left|W_2^{d_j} f[n_i]\right| \geq \left|W_2^{d_j} f[n_i + 1]\right| \tag{20}$$

And the equal sign cannot be taken in the two formulas at the same time, it is said that the wavelet coefficient has a modulus maximum at n points. The scale changes from large to small, and its modulus maximum will form a modulus maximum line.

The basic basis for detecting singular point mutations in time series based on wavelet transform modulus maxima is that the modulus maxima of wavelet transform on different scales of time series retain and highlight the most important information in the time series. The set of modulus maxima is a set of wavelet coefficients, which can be seen as discrete sampling of wavelet coefficients in a specific sense.

The noise and signal in the time series have different propagation characteristics when the wavelet transform is performed at the same time. That is, as the scale increases, the modulus maximum value corresponding to the noise increases, while the modulus maximum value of the signal decreases. Therefore, after several wavelet transforms are performed continuously, the modulus maximum corresponding to the noise has basically disappeared or the amplitude is small, and the remaining extreme points are mainly controlled by the signal. Based on this principle, we get the specific steps of the singular point location method of financial time series

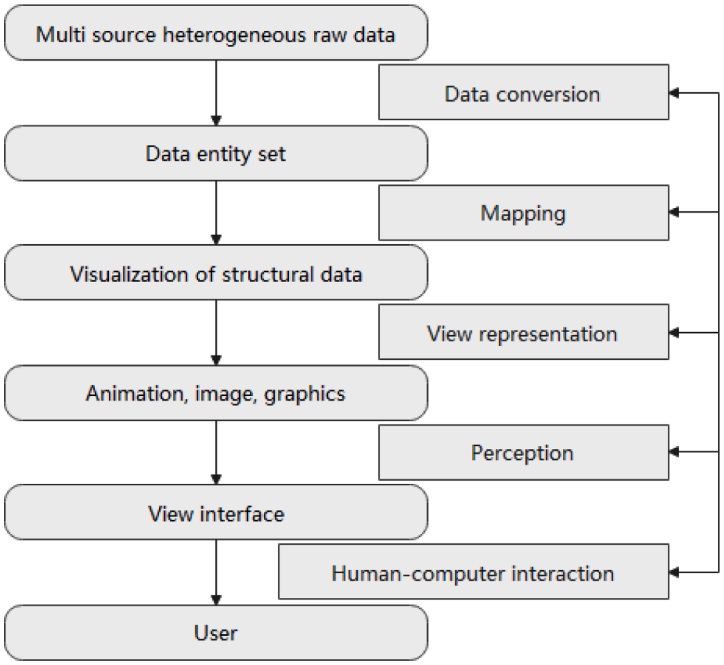

Fig. 3. Visual process model diagram.

based on the wavelet transform modulus maximum method.

Step1: The algorithm uses the selected wavelet (sym wavelet) to perform dyadic wavelet transformation on the processed time series. Generally, 4 to 5 decomposition scales are selected, and the modulus maximum value on each scale is calculated.

Step2: The algorithm selects a threshold A from the maximum scale. If the absolute value of the amplitude corresponding to the extreme point is greater than A, it is retained, otherwise the point is removed, so that a new modulus maximum point on the maximum scale is obtained.

Step3: The algorithm finds the wavelet transform modulus maximum point on the scale j to confirm the propagation point on the decomposition scale $j-1(j=4)$. The method is for a modulus maximum value x_1 on the decomposition scale j, if it has the same sign as a modulus maximum value x_2 on the scale $j-2$, and the position is relatively close and has a larger amplitude, then x_2 is considered as the propagation point of x_1 until the algorithm ends at $j=2$.

Step 4: in the position where there is an extreme point when j = 2, the corresponding extreme point when j = 1 is retained.In this way, the modulus maximum line of the signal can be found, and the singularity of the time series can be located on a precise scale.

For the selection principle of scale, theoretically, the maximum scale that can be selected is $j=\lfloor lbN \rfloor$, where the operator represents the round-down operation. However, in actual calculations, it is not necessary to take too large. Generally, 4 or 5 scales are selected, and the details may need to be determined according to specific problems. In fact, the larger the J, the more obvious the different characteristics of the noise and signal performance in the time series, and the more conducive to the separation of signal and noise. However, on the other hand, for reconstruction, the more wavelet decomposition, the greater the distortion, that is, the greater the reconstruction error. Therefore, when choosing the value of J, we should consider both to choose a moderate value.

The principle of threshold selection. Generally, we take the threshold as:

$$A = \max\left[W_2^{d_j} f[n_i]\right] \Big/ J \tag{21}$$

But it has the following shortcomings: 1) If the signal is given, A is basically fixed, and it does not reflect the relationship between threshold and noise. 2) If the value of A is too large, it will cause too much useful signal loss in the time series. However, if A is too small, the noise has not been cleaned up. Therefore, we believe that the selection of A should in principle be related to the specific characteristics of the signal and noise. All in all, the selection of threshold A should be based on the specific characteristics of the signal and noise, that is, different thresholds A should be adaptively selected.

Choice of the field of spreading point. The commonly used method of selecting the propagation point is $|x-x_0| \le C \cdot 2^j$. Among them, C is a positive number, and j is the decomposition scale. However, the disadvantage of the cone field is that when the selection scale is larger, the corresponding field will be larger. If there are too many candidate propagation points in the range, it is difficult to determine the modulus maximum corresponding to the real signal in the time series. In fact, the selection of the propagation point should be restricted by the point neighborhood. When the scale is larger, the point neighborhood is slightly enlarged. However, when the scale is small, the point neighborhood can be small. This can avoid the phenomenon of too many candidate propagation points.

The mutation point is an important feature to describe a transient signal. How to detect the signal mutation point has practical

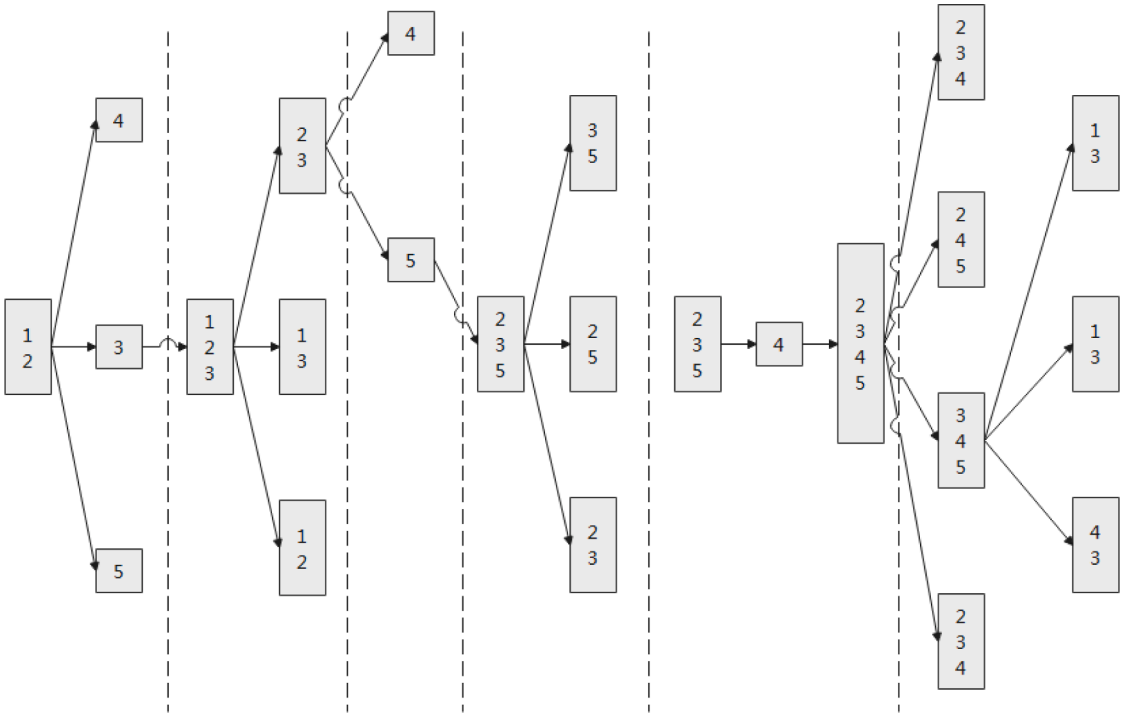

Fig. 4. Schematic diagram of the selection principle of time series variables.

significance. The wavelet transform has a close relationship with the exponent that characterizes the singularity of the time series, so the position of the singularity of the time series can be determined by the wavelet transform.

Theorem 1. When $0 \le \alpha \le 1$, the necessary and sufficient condition for the function $f(x)$ to have a consistent *Lipschitz* index α on $[a,b]$ is that there is a constant $k > 0$ such that $\forall_x \in [a,b]$, and the wavelet transform satisfies:

$$|W_{2^j} f(x)| \le k\left(2^j\right)^{\alpha} \tag{22}$$

If $f(x)$ is not *Lipschitz*1 at x_0, then $f(x)$ is said to be singular at x_0. If $f(x)$ is discontinuous but bounded at x_0, that is, $f(x)$ is discontinuous at x_0, then its *Lipschitz* index is 0.

Therefore, the *Lipschitz* index α describes the smoothness of $f(x)$ at point x_0. The larger the value of α, the smoother the function and the smaller the singularity. Conversely, the smaller the value of α, the sharper the change at that point and the greater the singularity.

Theorem 2: n is a positive number, $\varphi(x)$ is a wavelet function with compact support, and it has n-th order vanishing moments and n-th order is continuously differentiable. Then if there is a scale $s_0 > 0$ such that $|Wf(s,x)|$ is no local maximum for all $s < s_0$, $x \in [a,b]$, then there is uniform *Lipschitz*α on the interval $[\alpha - \varepsilon, \alpha + \varepsilon]$.

The theorem shows that if the wavelet change has no local maximum, then there is no singularity in any field. All the singular points of $f(x)$ can be located along the wavelet change modulus maximum line. After the singular points are located on a large scale, they should be accurately located step by step on a smaller scale. The modulus maxima of wavelet transform of time series at different scales contain the most important information in the information, which is the basic basis for signal mutation detection based on modulus maxima.

4. Regional economic visualization system based on time series

This article combines machine learning and time series to construct a regional economic visualization system. The visualization process modeling is shown in Figure 3. The visualization process first starts with multi-source heterogeneous raw data, and then mines and processes it into multi-source heterogeneous data sets. Then, the data set is visually mapped to data with a visual structure. Secondly, the visual structure is expressed through views and displayed in animations, images and images on computers, mobile smart terminals or smart terminals. Finally, it uses sensory organs to perceive the computer, mobile smart terminal or smart terminal view interface to obtain information and conduct appropriate interactions. Visual mapping is the focus of the visualization model, which converts diverse and heterogeneous data into animations, images and graphics suitable for the human perception system. The mapping process includes the expression of texture, color, size, shape, and orientation of animation, images and graphics.

The selection method of spatial and temporal geographic weighted variables based on stepwise regression is to judge the choice of variables multiple times. After a variable is introduced into the model, it may be deleted because the later introduced variable affects

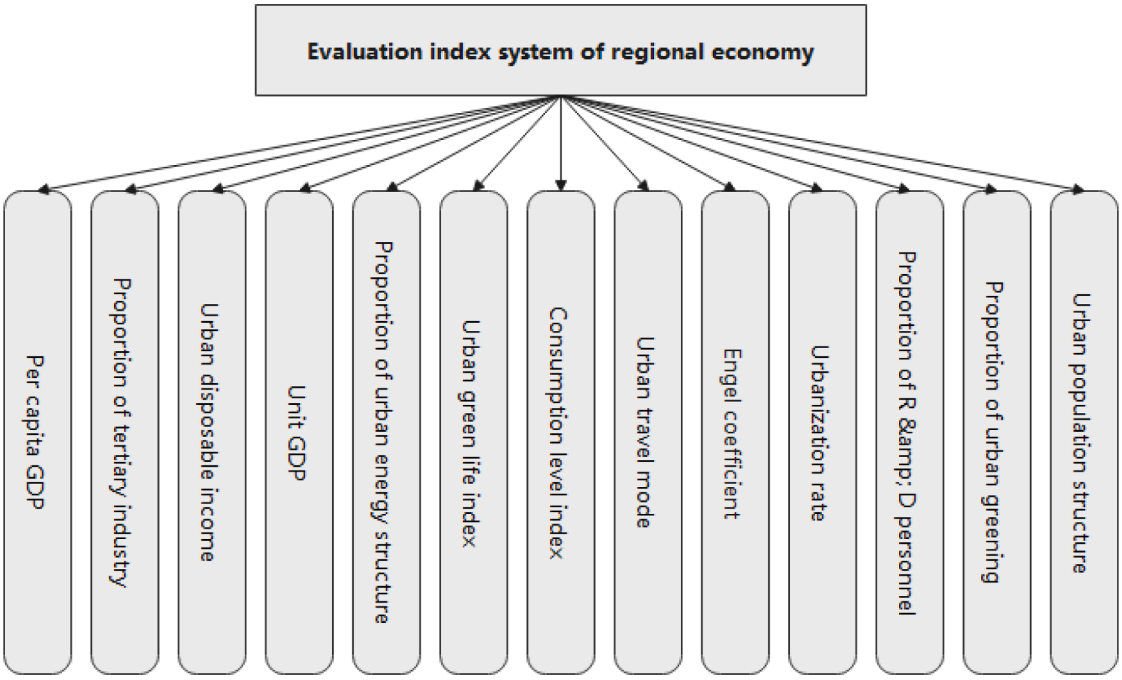

Fig. 5. Regional economic evaluation index system.

its significance. Therefore, the model established by the time series weighted variable selection method based on stepwise regression is the global optimal model. Figure 4 takes 5 variables (initialized pre-selected variables are 2 variables) as an example to illustrate the principle of the selection method of spatial and temporal geographic weighted variables based on stepwise regression.

This article attempts to establish an evaluation index system that can reflect the four aspects of economic development, scientific and technological progress, social development and environment. It can not only statically reflect the current regional economic development, but also dynamically reflect the changes in this paper. Under the guidance of the development requirements of "regional economic goals" and "low-carbon cities", according to the selected index factors in the city's low-carbon comprehensive evaluation index system, after considering the difficulty of quantifying qualitative indexes, the regional economic evaluation index system of this paper is finally constructed, as shown in Figure 5.

The design of the visual analysis system for regional economic data analysis should meet the needs of the actual work of economic analysis, reduce the work pressure of economic analysis, improve the accuracy of economic analysis, and be applicable to the practice of economic analysis. In general, the following goals need to be achieved:

In terms of improving data quality, the visual analysis system needs to do two things well. One is to establish a data entry-review mechanism. When the analysis unit enters the data, the system will automatically judge the matching of the basic data according to the nature of the unit. After the data is submitted, the statistics department will judge its authenticity based on the historical data. The second is to reduce the chance of error. The analysis system can reduce the link of manual data collection and then entering the electronic form, thereby avoiding the distortion of the data due to human operation errors.

According to the processing flow and processing rules of the economic analysis work, as well as the function points that the analysis database system should have, the overall function point integration of the interface can be obtained as shown in Figure 6.

This article uses a standard three-tier architecture to implement the B/S (browser/server) model. The three-tier architecture is centered on data access, HTTP is the data transmission protocol, and multi-level servers are established to realize the rapid exchange of data between the browser and the server and improve the response speed of the system. The three-tier architecture is shown in Figure 7.

When constructing the visualization platform for regional economic evaluation, in order to realize the process from basic data of regional economic indicators to model data and then to visualization, the visualization platform is divided into four management systems: basic data management, model management, visual display management, and system management, as shown in Figure 8.

According to the module structure of the regional economic assessment visualization platform, the functions of the platform are implemented in the path from the basic database to the model database, and the model data integration layer to the visualization display, as shown in Figure 9.

The basic database is responsible for the input, query, analysis, and export of basic data. The model database is responsible for the input, query, analysis, and export of model data obtained from the basic data through the data processing layer. The data integration layer uses the data and weights obtained from the data processing layer to complete the horizontal regional economic evaluations at the national, regional, provincial, and city levels, as well as the vertical regional economic evaluations within the specified time series

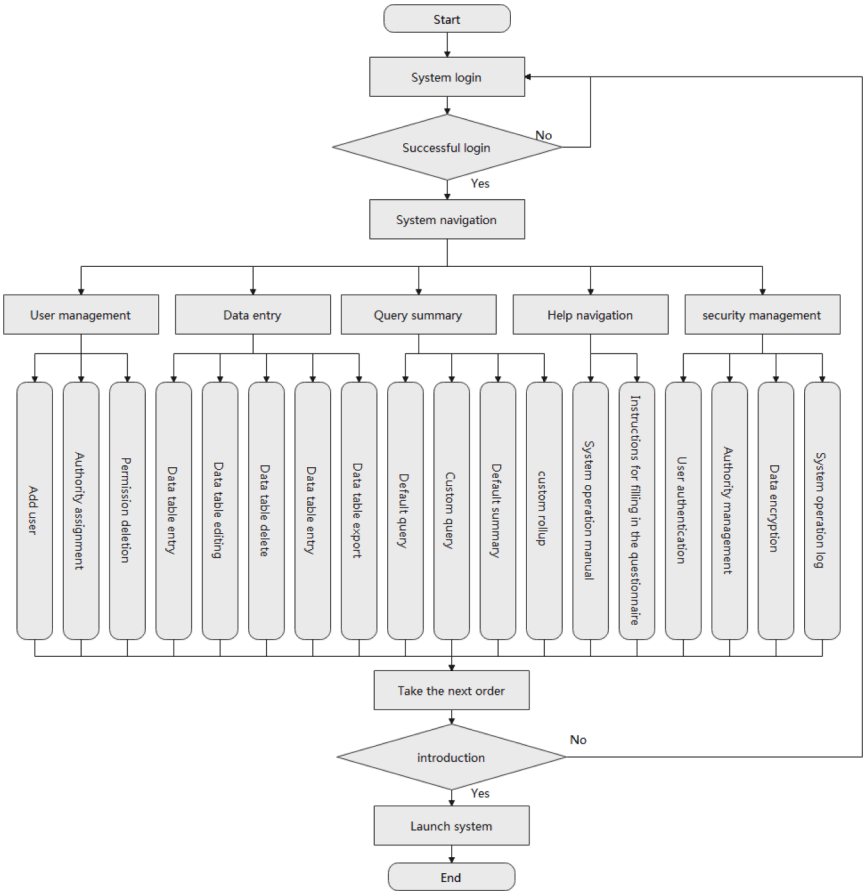

Fig. 6. Summary of the overall function points of the interface.

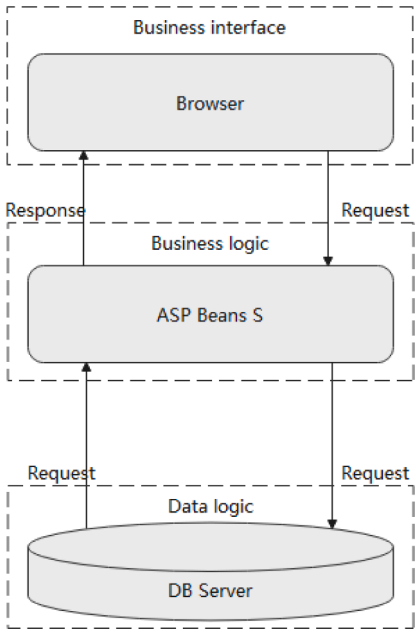

Fig. 7. System architecture diagram.

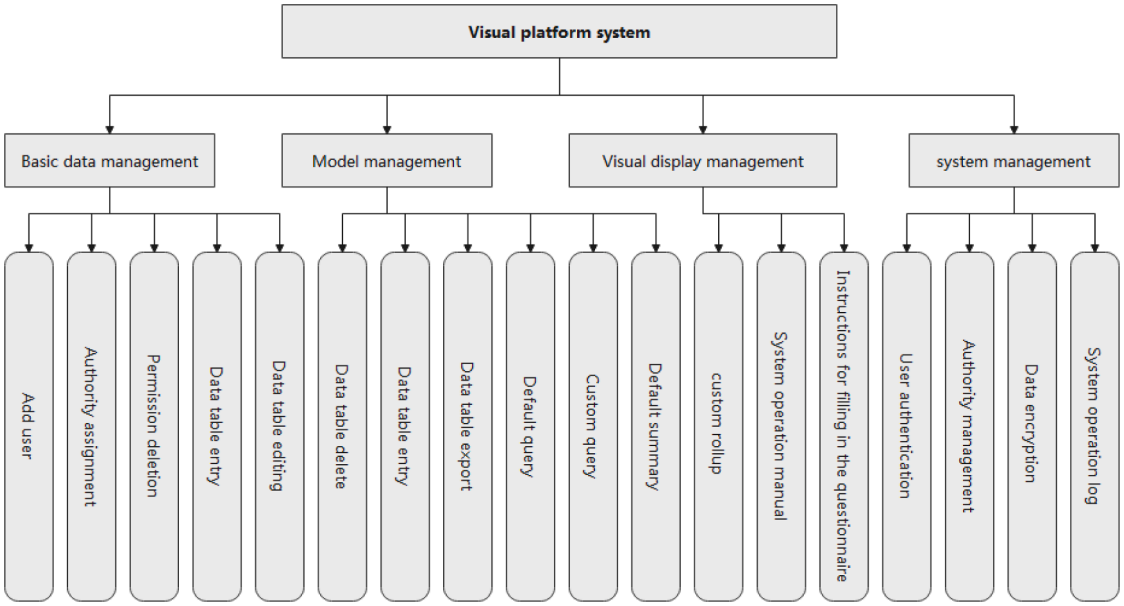

Fig. 8. The management system of the regional economic assessment visualization platform.

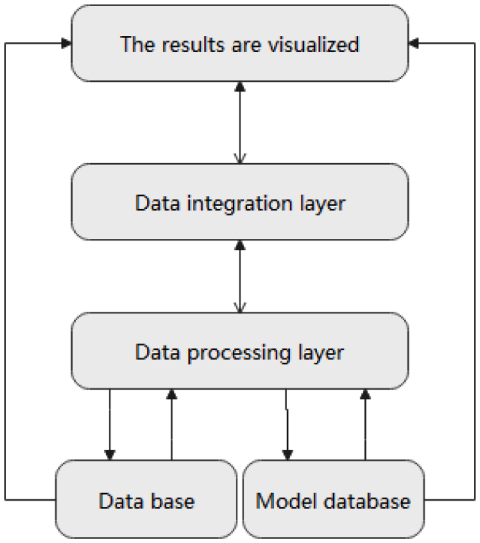

Fig. 9. The implementation path of the visualization platform of regional economic development level assessment.

of each specific geographic level. The result display visualization layer is responsible for the visual display of the low-carbon assessment results. Refer to Figure 10 for the architecture diagram of the system. In addition, through the design of the import module, users can directly import the original data files of different formats into the relational database, such as a large number of EXCEL tables. Similarly, the design of the data backup module allows users to back up data in relational databases and geographic data in MapInfo into data files in different formats.

Application data caching technology can solve the problem of spatial data access efficiency in the application of the system to a certain extent, thereby increasing the system information query rate. The system uses a client data caching system to establish a local mirror of part of the data in the database, and organize such data on the local storage in a certain way, that is, a strategy of using storage space to exchange speed. The specific principle is shown in Figure 11.

5. Testing of the regional economic visualization analysis system based on time series

After constructing a time-series-based regional economic visualization analysis system, it is necessary to evaluate the performance

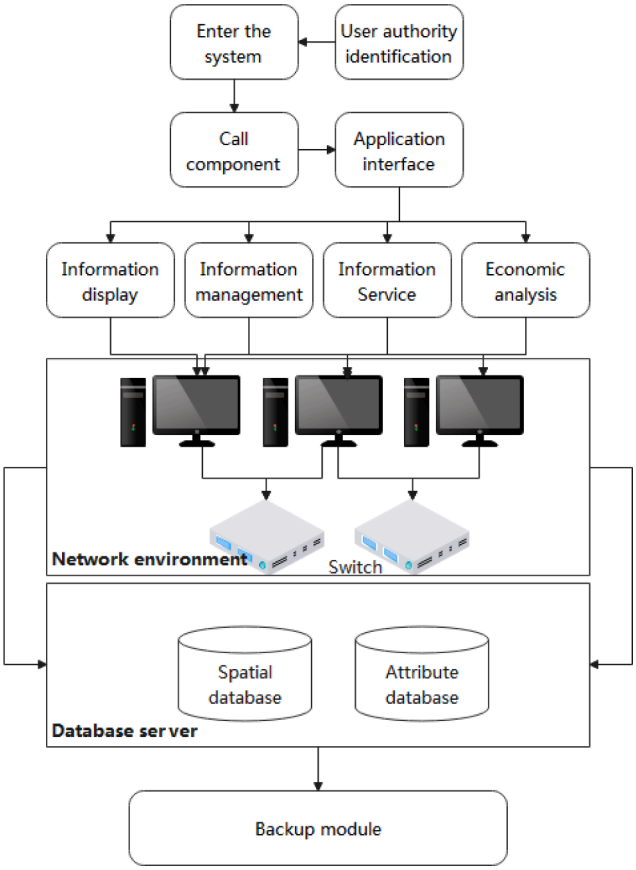

Fig. 10. System logical structure diagram.

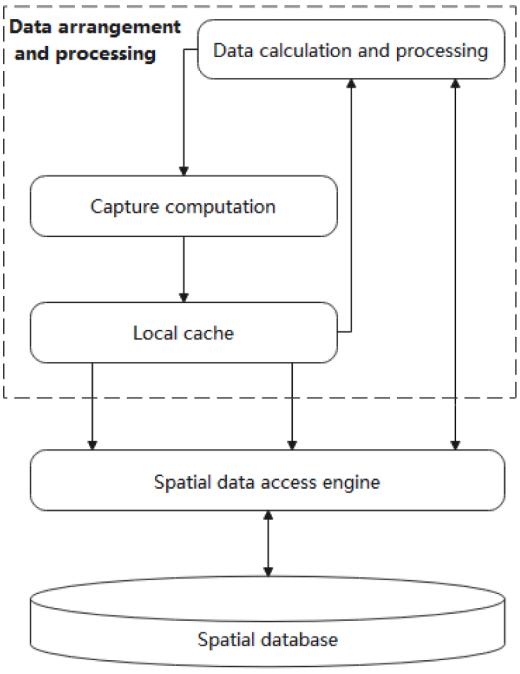

Fig. 11. Principle of data processing.

Table 1
Statistical table of the economic data analysis effect of the regional economic visualization system based on time series

No.	Data analysis	No.	Data analysis	No.	Data analysis	No.	Data analysis
1	90.5	26	91.9	51	82.2	76	86.4
2	85.5	27	81.5	52	82.9	77	84.6
3	86.9	28	88.2	53	89.9	78	86.4
4	84.7	29	87.1	54	85.9	79	92.5
5	88.8	30	92.7	55	84.4	80	80.1
6	92.7	31	91.8	56	84.8	81	87.5
7	89.7	32	81.4	57	86.9	82	86.6
8	81.5	33	84.9	58	85.9	83	88.9
9	90.4	34	82.9	59	91.3	84	88.5
10	92.8	35	86.7	60	91.3	85	79.8
11	90.4	36	87.3	61	88.4	86	86.7
12	79.7	37	82.7	62	90.3	87	84.2
13	90.6	38	85.7	63	92.0	88	90.2
14	85.0	39	81.9	64	81.7	89	80.0
15	84.6	40	79.3	65	82.5	90	90.8
16	81.6	41	80.2	66	91.7	91	90.2
17	89.9	42	82.0	67	87.5	92	84.2
18	85.1	43	85.0	68	84.3	93	82.9
19	89.4	44	92.2	69	82.2	94	81.8
20	86.3	45	83.2	70	81.8	95	90.6
21	90.1	46	82.4	71	87.0	96	82.0
22	84.2	47	79.8	72	84.8	97	82.0
23	85.9	48	81.9	73	86.8	98	79.8
24	84.0	49	92.5	74	92.5	99	81.0
25	85.0	50	89.8	75	92.2	100	93.0

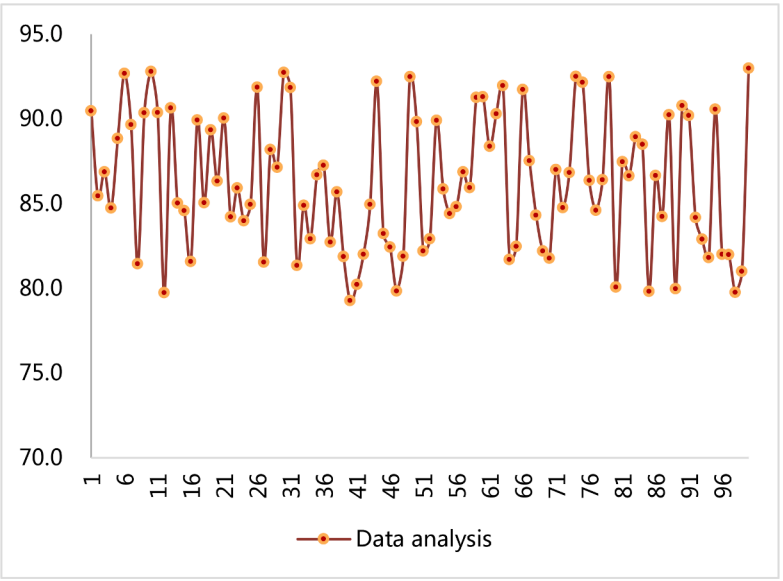

Fig. 12. Statistical diagram of the economic data analysis effect of the regional economic visualization system based on time series.

of the system and study the effectiveness of the system model in regional economic analysis. The time series in this paper is based on machine learning, and data training and data learning are carried out through time series, and data is sorted through time series, which can effectively improve the effect of data learning and forecasting. This paper designs an experiment based on a certain regional economy to verify the system's regional economic time series analysis effect and visual analysis effect.

First, this paper evaluates the economic data analysis effect of the model constructed in this paper. Moreover, this paper mainly uses regional economic data as an example to conduct data analysis through system simulation, and the results of economic data analysis are shown in Table 1 and Figure 12.

On the basis of the above analysis, the system visualization effect evaluation is carried out, the test results are counted and the statistical graphs are drawn, as shown in Table 2 and Figure 13.

From the results of the experimental research, the regional economic visualization system based on time series constructed in this paper has perfect system functions and can meet the needs of regional economic analysis.

Table 2
Statistical table of the visualization effect evaluation of the regional economic visualization system based on time series

No.	Visual evaluation	No.	Visual evaluation	No.	Visual evaluation	No.	Visual evaluation
1	83.3	26	86.6	51	89.9	76	87.3
2	90.3	27	84.9	52	84.0	77	89.4
3	87.4	28	90.2	53	89.5	78	88.0
4	83.1	29	90.4	54	85.5	79	85.7
5	88.1	30	87.8	55	85.2	80	84.0
6	89.0	31	88.0	56	89.8	81	83.5
7	83.8	32	84.1	57	84.4	82	84.7
8	89.3	33	90.4	58	87.4	83	85.8
9	86.1	34	90.4	59	85.3	84	88.3
10	88.0	35	87.4	60	85.6	85	90.9
11	88.3	36	90.8	61	85.3	86	89.8
12	83.7	37	84.0	62	89.5	87	86.5
13	88.8	38	89.3	63	86.4	88	85.3
14	86.6	39	88.7	64	84.5	89	84.8
15	87.4	40	89.9	65	88.2	90	89.3
16	90.7	41	90.4	66	90.2	91	89.7
17	83.5	42	87.5	67	89.1	92	91.0
18	85.7	43	85.1	68	87.5	93	89.0
19	88.9	44	88.1	69	85.2	94	87.5
20	87.9	45	85.6	70	85.2	95	87.4
21	84.9	46	84.9	71	85.8	96	85.9
22	89.6	47	83.2	72	90.2	97	85.0
23	86.7	48	89.8	73	83.1	98	83.3
24	84.2	49	88.2	74	89.9	99	90.4
25	89.2	50	86.7	75	83.7	100	85.3

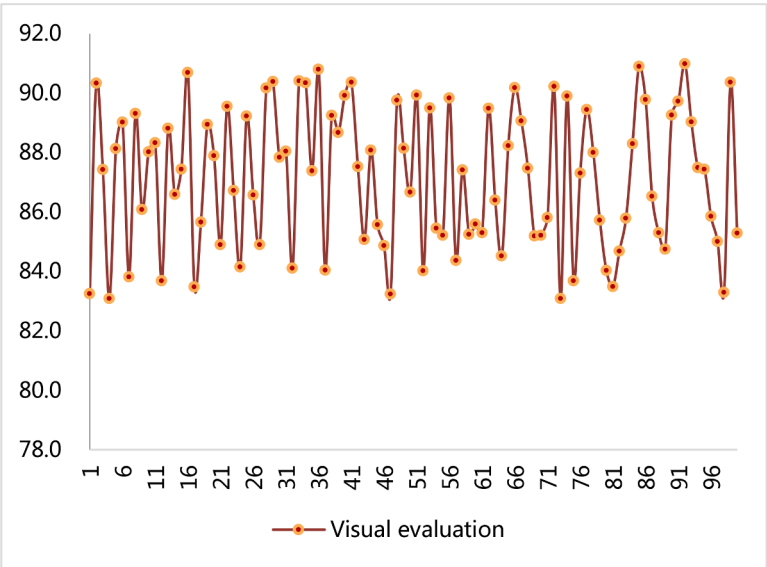

Fig. 13. Statistical diagram of the visualization effect evaluation of the regional economic visualization system based on time series

6. Conclusion

This article provides service encapsulation, scientific analysis and simple operation of regional economic visualization analysis data from three levels: database storage, intelligent data analysis methods, and data visualization presentation. Moreover, this paper uses machine learning algorithms to analyze time series data, uses various models and methods of intelligent data analysis to mine data laws from huge data, and counts data reports to find problems in economic development. The key to data object visualization is to determine the correspondence between data objects and visualization objects, that is, the mapping relationship between data space and image space. The visualization of the evaluation process uses the evaluation algorithm to determine the data objects and parameters, and embeds the visualization technology into the evaluation process to achieve a visual display. Finally, after the system is built, this paper tests the system performance. From the results of the experimental research, it can be seen that the regional economic visualization system based on time series constructed in this paper has perfect system functions and can meet the needs of regional

economic analysis.

Author statement

Yang Bai and Min Zhao worked together on this article, with Rong Li mainly responsible for model design and program development and Peizhu Xin responsible for writing and submitting the manuscript.

References

Montford, W, & Goldsmith, R. E. (2016). How gender and financial self-efficacy influence investment risk taking[J]. *International Journal of Consumer Studies, 40*(1), 101–106.

Wanjohi, S M, Wanjohi, J G, & Ndambiri, J M (2017). The effect of financial risk management on the financial performance of commercial banks in Kenya[J]. *International Journal of Finance and Banking Research, 3*(5), 70–81.

Magendans, J, Gutteling, J M, & Zebel, S. (2017). Psychological determinants of financial buffer saving: the influence of financial risk tolerance and regulatory focus [J]. *Journal of risk research, 20*(8), 1076–1093.

Cole, E S, Walker, D, Mora, A, et al. (2014). Identifying hospitals that may be at most financial risk from Medicaid disproportionate-share hospital payment cuts[J]. *Health Affairs, 33*(11), 2025–2033.

Zalik, A. (2015). Resource sterilization: reserve replacement, financial risk, and environmental review in Canada's tar sands[J]. *Environment and Planning A, 47*(12), 2446–2464.

Lucarelli, C, Uberti, P, & Brighetti, G. (2015). Misclassifications in financial risk tolerance[J]. *Journal of Risk Research, 18*(4), 467–482.

Chan, E Y (2015). Physically-attractive males increase men's financial risk-taking[J]. *Evolution and Human Behavior, 36*(5), 407–413.

West, T, & Worthington, A C (2014). Macroeconomic conditions and Australian financial risk attitudes, 2001–2010[J]. *Journal of Family and Economic Issues, 35*(2), 263–277.

Tanimura, T, Jaramillo, E, Weil, D, et al. (2014). Financial burden for tuberculosis patients in low-and middle-income countries: a systematic review[J]. *European Respiratory Journal, 43*(6), 1763–1775.

Scharding, T K (2015). Imprudence and immorality: A Kantian approach to the ethics of financial risk[J]. *Business Ethics Quarterly, 25*(2), 243–265.

Su, J, & Furman, E (2017). A form of multivariate Pareto distribution with applications to financial risk measurement[J]. *ASTIN Bulletin: The Journal of the IAA, 47*(1), 331–357.

Guo, H., Guo, C., Xu, B., et al. (2021). MLP neural network-based regional logistics demand prediction. *Neural Comput & Applic, 33*, 3939–3952.

Karanikić, Petra, Mladenović, Igor, Sokolov-Mladenović, Svetlana, et al. (2019). Retraction Note: Prediction of economic growth by extreme learning approach based on science and technology transfer[J]. *Quality & Quantity, 53*(2), 1095–1096.

Ataka, Kazuto (2014). Prediction of Election Result and Economic Indicator[J]. *resuscitation, 96*(6), 84-84.

Barde, S (2015). Back to the Future: Economic Self-Organisation and Maximum Entropy Prediction[J]. *Computational Economics, 45*(2), 337–358.

Ferramosca, A, Limon, D, & Camacho, E F (2014). Economic MPC for a Changing Economic Criterion for Linear Systems[J]. *Automatic Control IEEE Transactions on, 59* (10), 2657–2667.

Zhou, L, Lai, K K, & Yen, J (2014). Bankruptcy prediction using SVM models with a new approach to combine features selection and parameter optimisation[J]. *International Journal of Systems Science, 45*(1-3), 241–253.

Bhattacharya, D, Mukhoti, J, & Konar, A (2019). Learning regularity in an economic time-series for structure prediction[J]. *Applied Soft Computing, 76*(2), 31–44.

Li, Shixuan, Shi, Wenxuan, Wang, Jiancheng, & Zhou, Heshen (2021). A Deep Learning-Based Approach to Constructing a Domain Sentiment Lexicon: a Case Study in Financial Distress Prediction. *Information Processing and Management, 58*(5), Article 102673.

Vu, H L, Ng, K T W, & Bolingbroke, D (2019). Time-lagged effects of weekly climatic and socio-economic factors on ANN municipal yard waste prediction models[J]. *Waste Management, 84*(2), 129–140.

Teljeur, C, O"Neill, M, Moran, P, et al. (2014). Using prediction intervals from random-effects meta-analyses in an economic model[J]. *International Journal of Technology Assessment in Health Care, 30*(01), 44–49.

Kleven, H J, & Schultz, E. A. (2014). Estimating taxable income responses using Danish tax reforms[J]. *American Economic Journal: Economic Policy, 6*(4), 271–301.

Hoffmann, M. (2014). The consumption–income ratio, entrepreneurial risk, and the us stock market[J]. *Journal of Money, Credit and Banking, 46*(6), 1259–1292.

Carvalho, L, & Di Guilmi, C. (2020). Technological unemployment and income inequality: a stock-flow consistent agent-based approach[J]. *Journal of Evolutionary Economics, 30*(1), 39–73.

Gantino, R. (2015). Effect of Managerial Ownership Structure, Financial Risk and Its Value on Income Smoothing in the Automotive Industry and Food & Beverage Industry Listed in Indonesia Stock Exchange[J]. *Research Journal of Finance and Accounting, 6*(4), 48–56.